

Final results on the $\pi/K/p$ production in pp and Pb—Pb collision at 5.02 TeV



Omar Vázquez

V Congreso de la Red Mexicana Científica y
Tecnológica para ALICE-LHC

28-09-2018

Outline

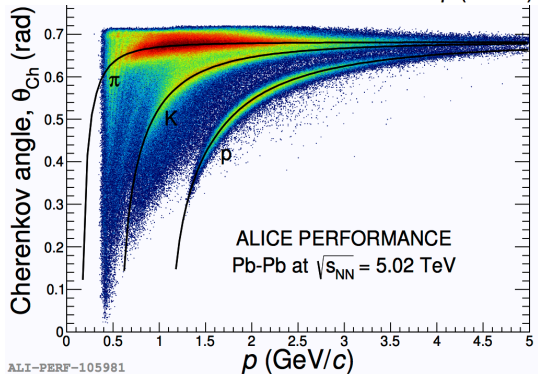
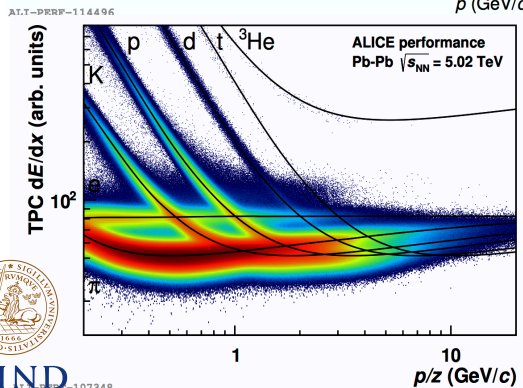
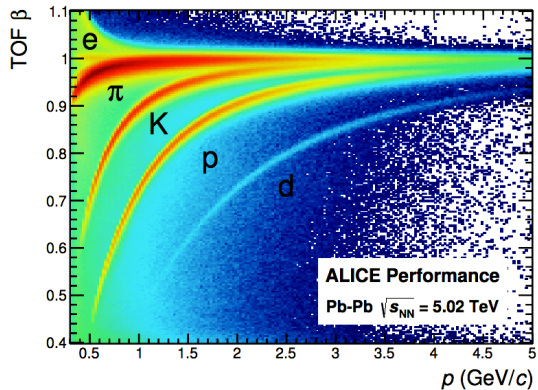
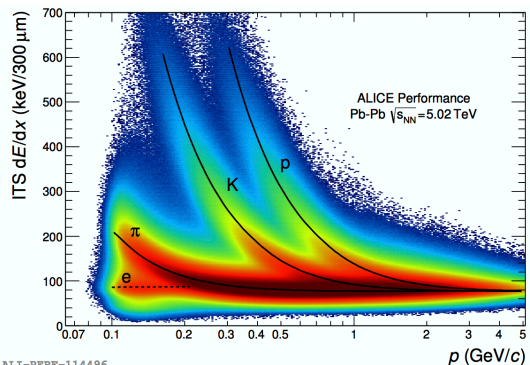
- Motivations
- PID with the TPC of ALICE
- Status of the paper: “Production of charged pions, kaons, (anti)protons in Pb—Pb and minimum bias pp collisions at 5.02 TeV”
- Conclusions

Motivations to do PID in ALICE

- The p_T distributions of $\pi/K/p$ allow to study the bulk properties and dynamical evolution on the created system in heavy-ion collisions.
- The high p_T spectra of hadrons ($> 10 \text{ GeV}/c$) can be used as proxies for jets to get insight into mechanisms of medium-induced energy loss.

Motivations to do PID in ALICE

- The p_T distributions of $\pi/K/p$ allow to study the bulk properties and dynamical evolution on the created system in heavy-ion collisions.
- The high p_T spectra of hadrons (> 10 GeV/c) can be used as proxies for jets to get insight into mechanisms of medium-induced energy loss.



π^\pm	K^\pm	$p(\bar{p})$
ITS		
0.1 - 0.8	0.2 - 0.6	0.3 - 0.8
TPC (low p_T)		
0.3 - 0.7	0.25 - 0.45	0.4 - 0.8
TPC (high p_T)		
3 - 12	4 - 12	4 - 12
TOF		
0.6 - 2.5	1.0 - 2.5	0.8 - 4
HMPID		
1.5 - 4	1.5 - 4	1.5 - 6
Kinks		
-	0.2-5.0	-
Measured in GeV/c		



$$\frac{d^2 N_{\bar{p}}}{dp_T dy} = J f_{\bar{p}} C_{\text{FD}} \left(C_{\text{Mat}} \frac{\epsilon_{\text{ch}}}{\epsilon_{\bar{p}}} \right) \times \left(\frac{d^2 N_{\text{ch}}}{dp_T d\eta} \frac{1}{\epsilon_{\text{ch}}} \right)_{|\eta| < 0.8}$$

*Example for \bar{p}

J : Jacobian transformation ($\eta \rightarrow y$)

$f_{\bar{p}}$: Particle abundances

C_{FD} : Feed-down correction

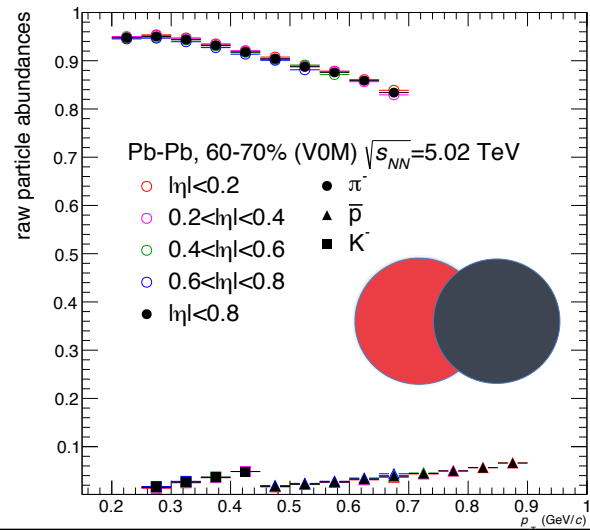
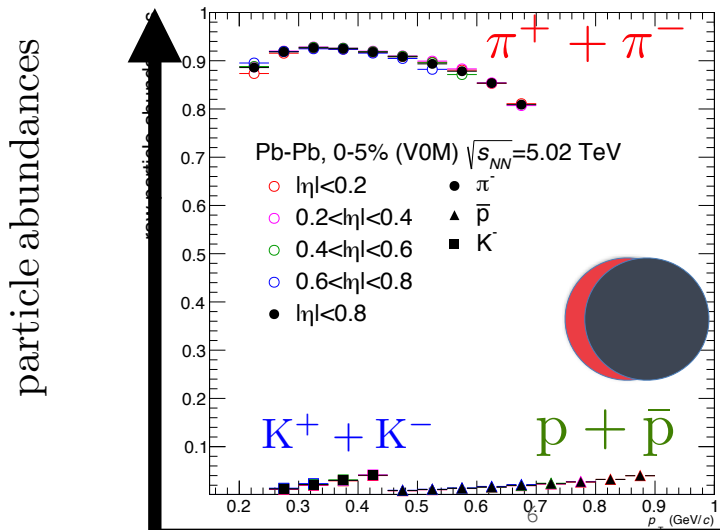
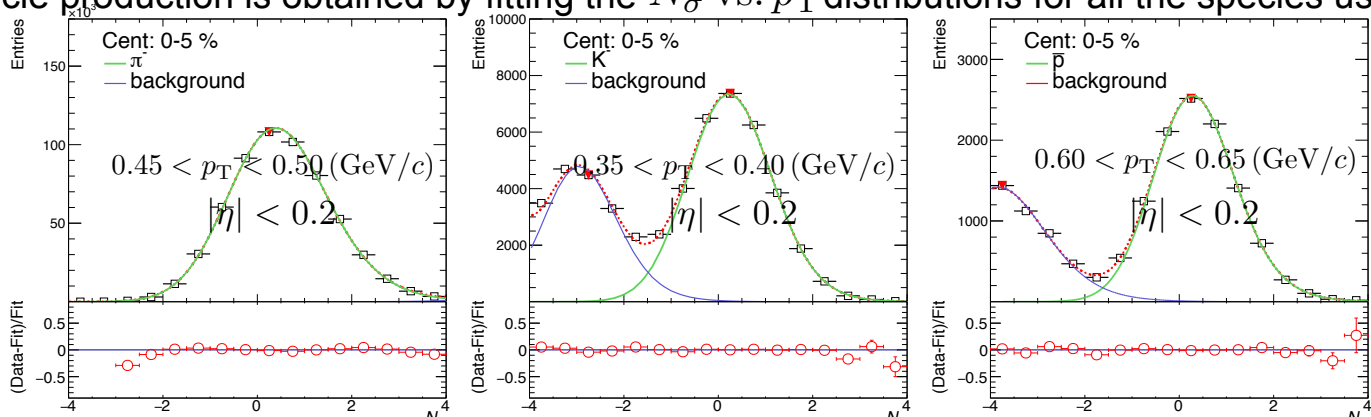
C_{Mat} : Geant-Fluka correction

$\frac{\epsilon_{\text{ch}}}{\epsilon_{\bar{p}}}$: Relative efficiency correction

$\frac{d^2 N_{\text{ch}}}{dp_T d\eta}$: Inclusive charged particle p_T spectrum

Low p_T analysis

The particle production is obtained by fitting the N_σ vs. p_T distributions for all the species using a 2-Gaussian function

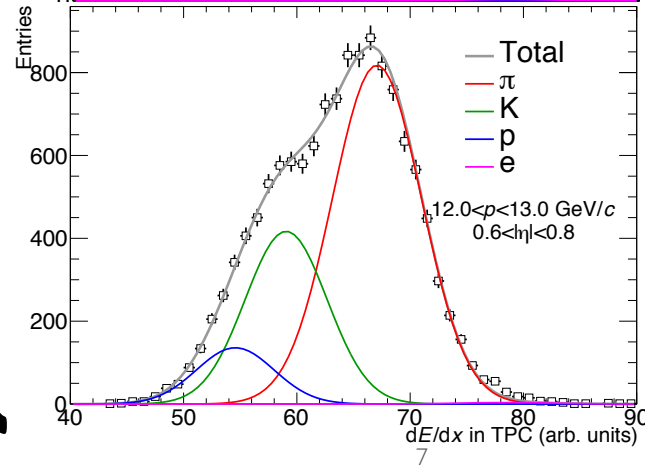
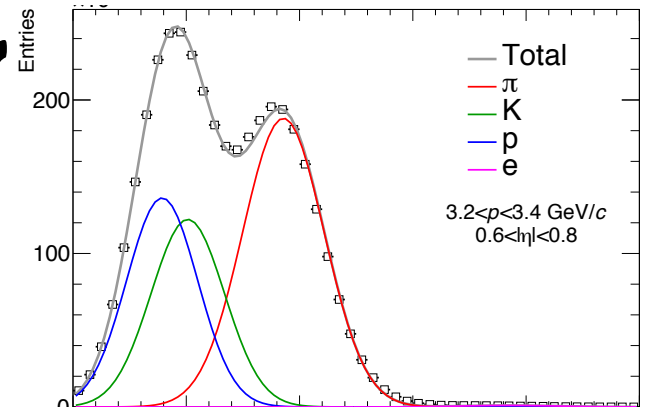
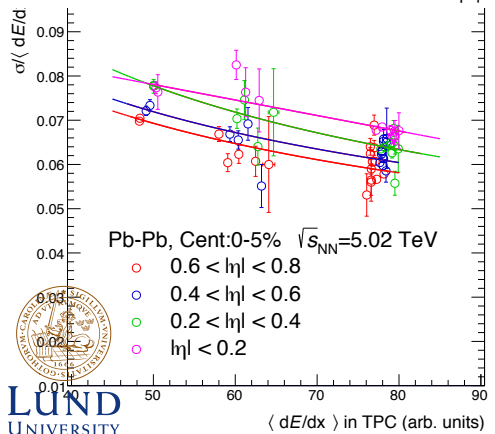
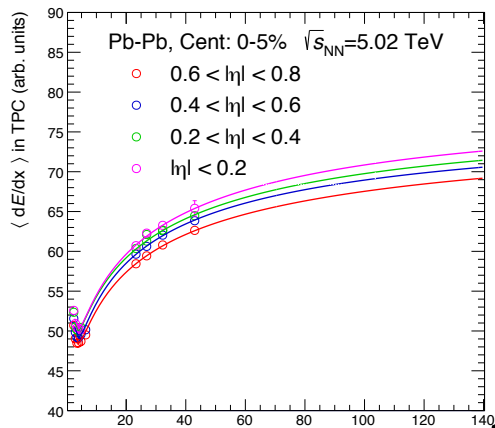


p_T



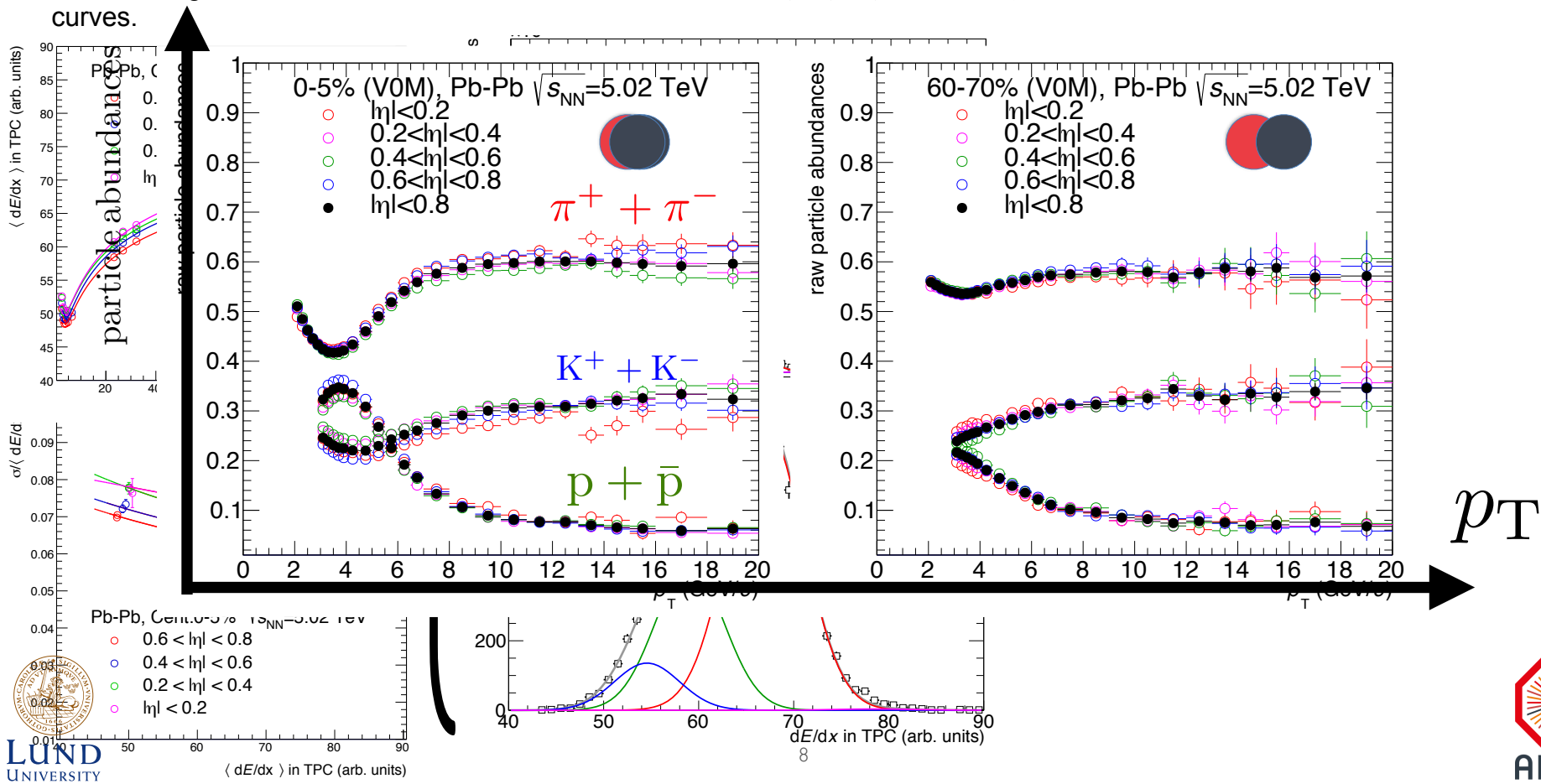
High p_T analysis

1. The extraction of the yields begins with the parameterization of the Bethe-Bloch and resolution curves.
2. The TPC signal is fitted to a four-Gaussian function, in which $\langle dE/dx \rangle$ and $\sigma \langle dE/dx \rangle$ are extracted from the BB and resolution curves.

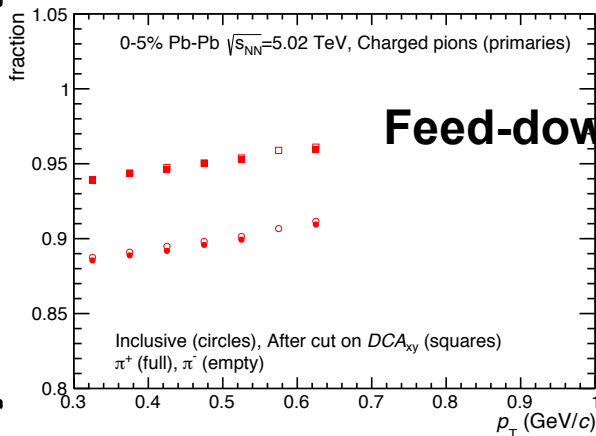
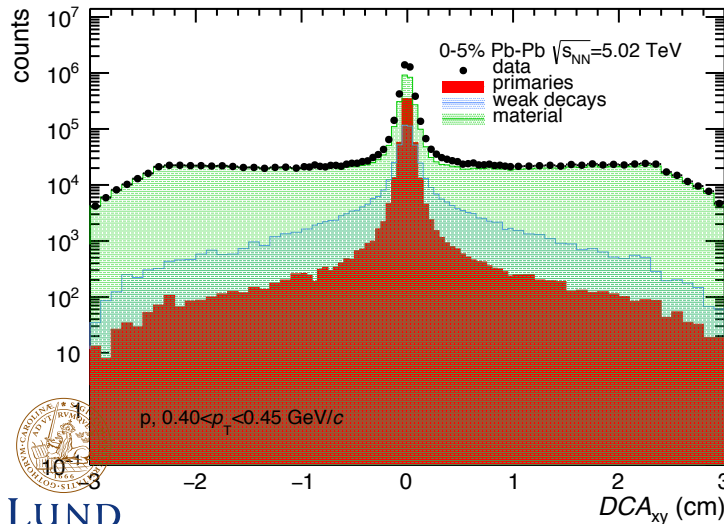
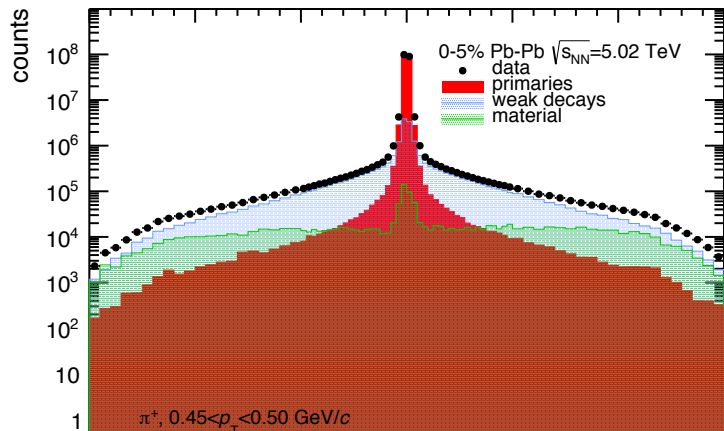


High p_T analysis

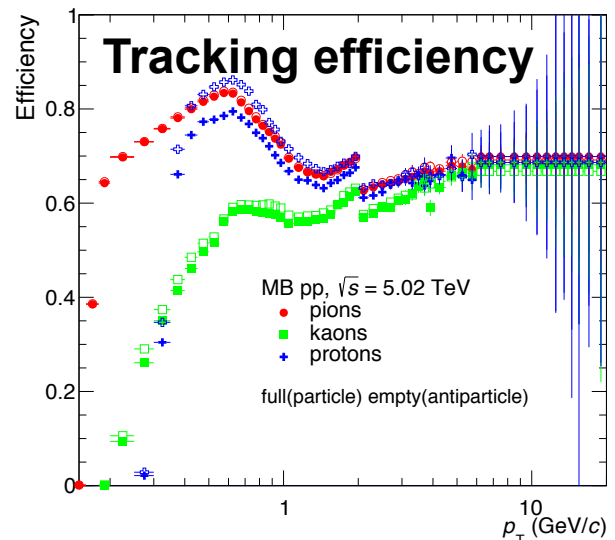
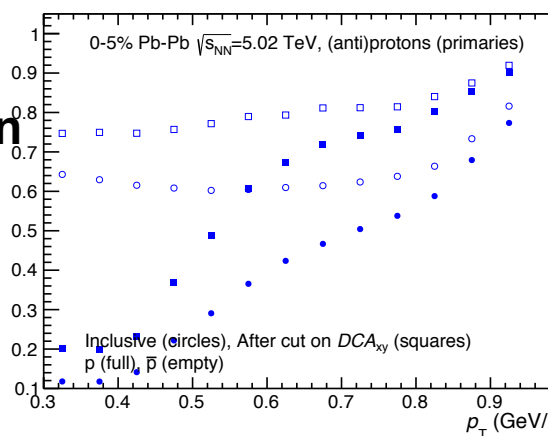
1. The extraction of the yields begins with the parameterization of the Bethe-Bloch and resolution curves.
2. The TPC signal is fitted to a four-Gaussian function, in which $\langle dE/dx \rangle$ and $\sigma \langle dE/dx \rangle$ are extracted from the BB and resolution curves.



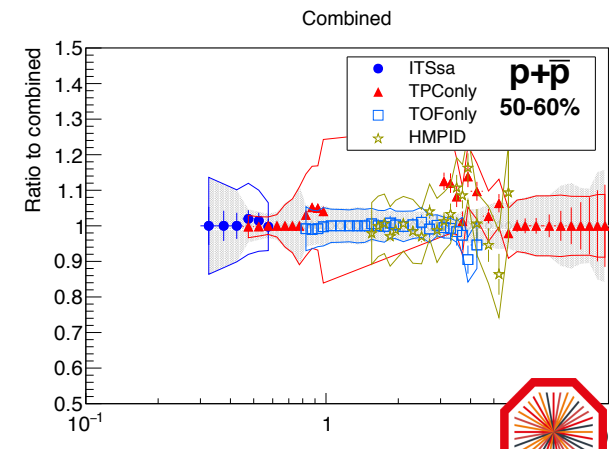
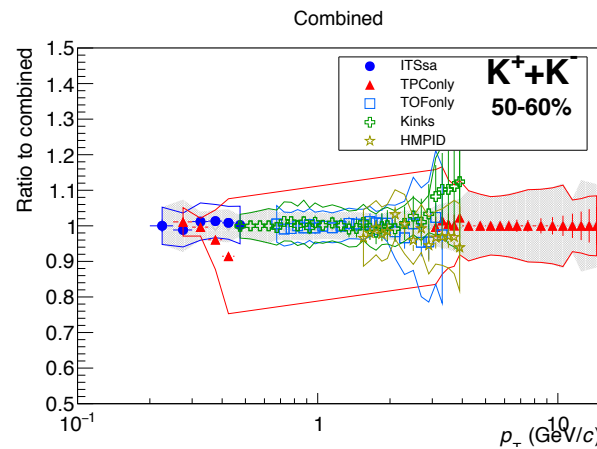
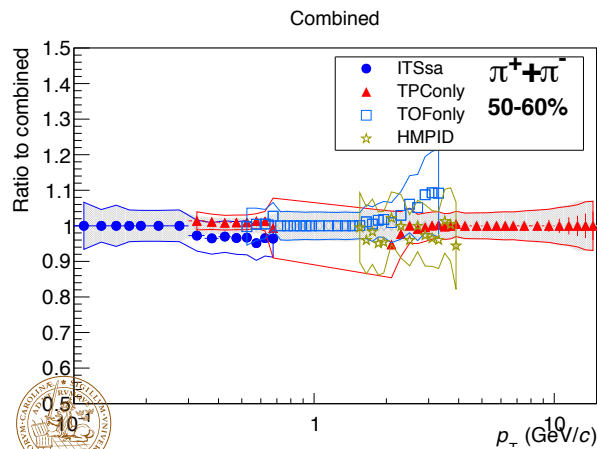
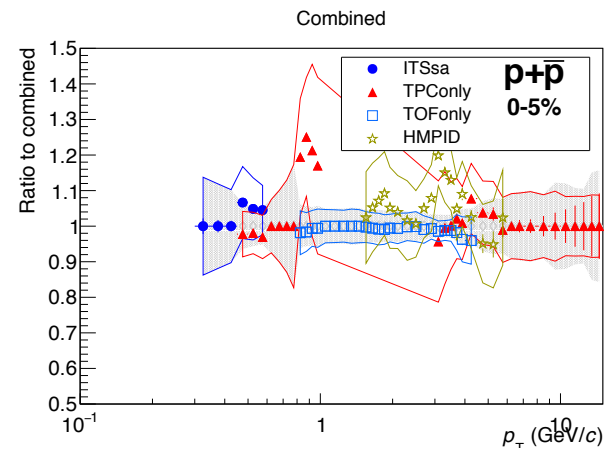
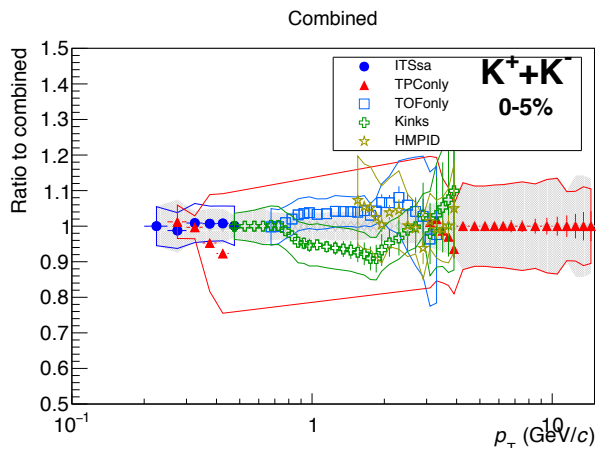
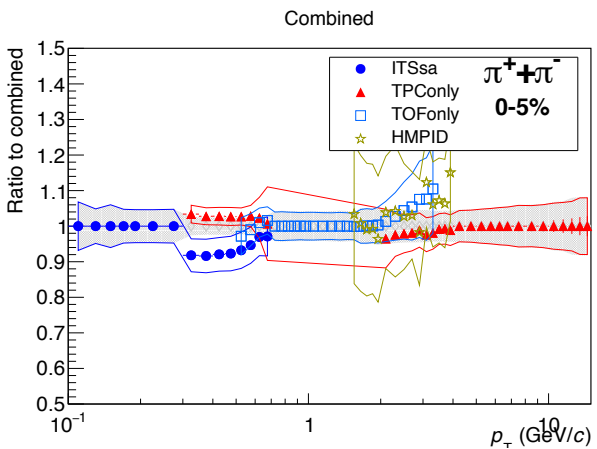
Corrections



Feed-down

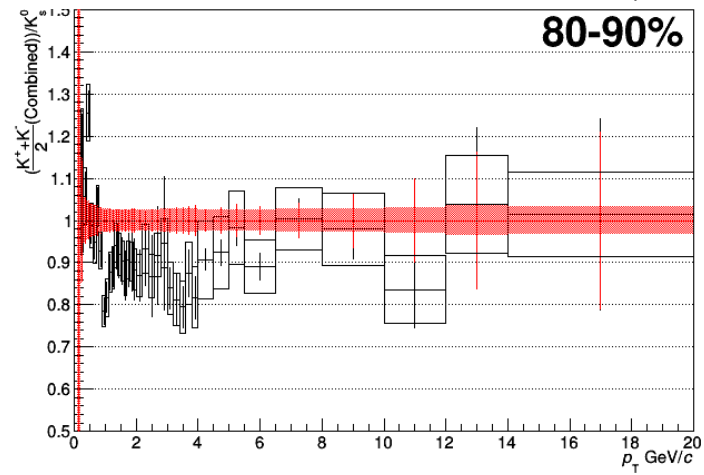
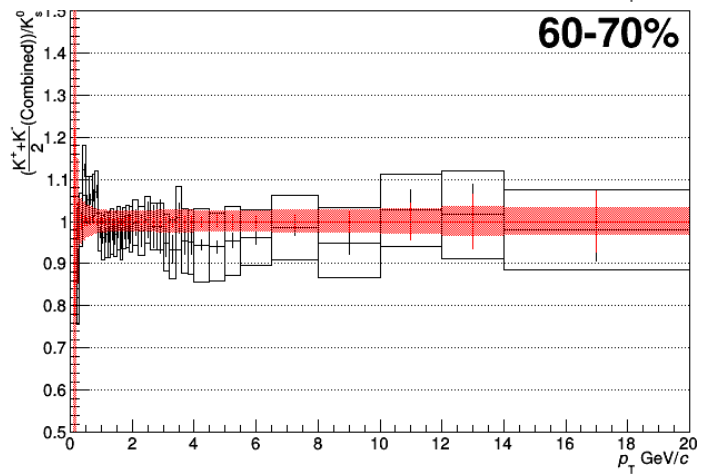
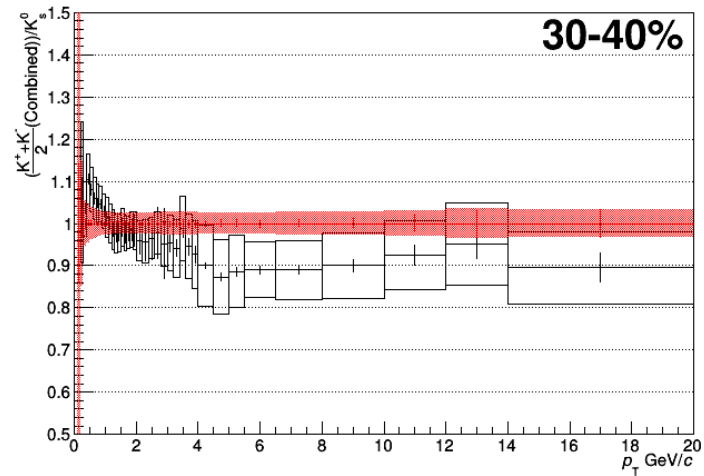
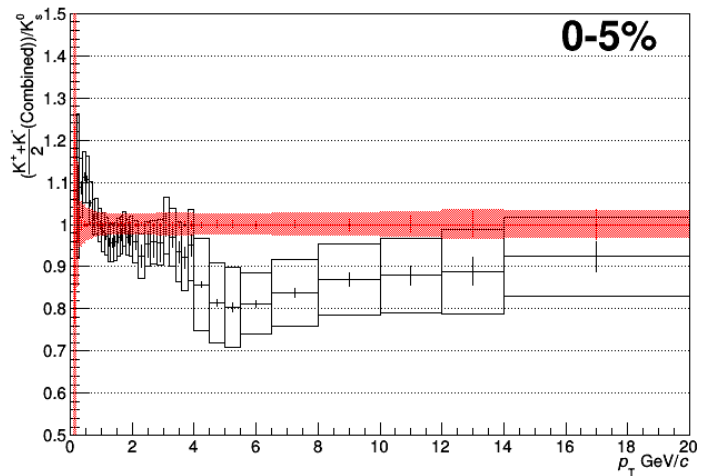


Comparison of individual analysis to combined spectra

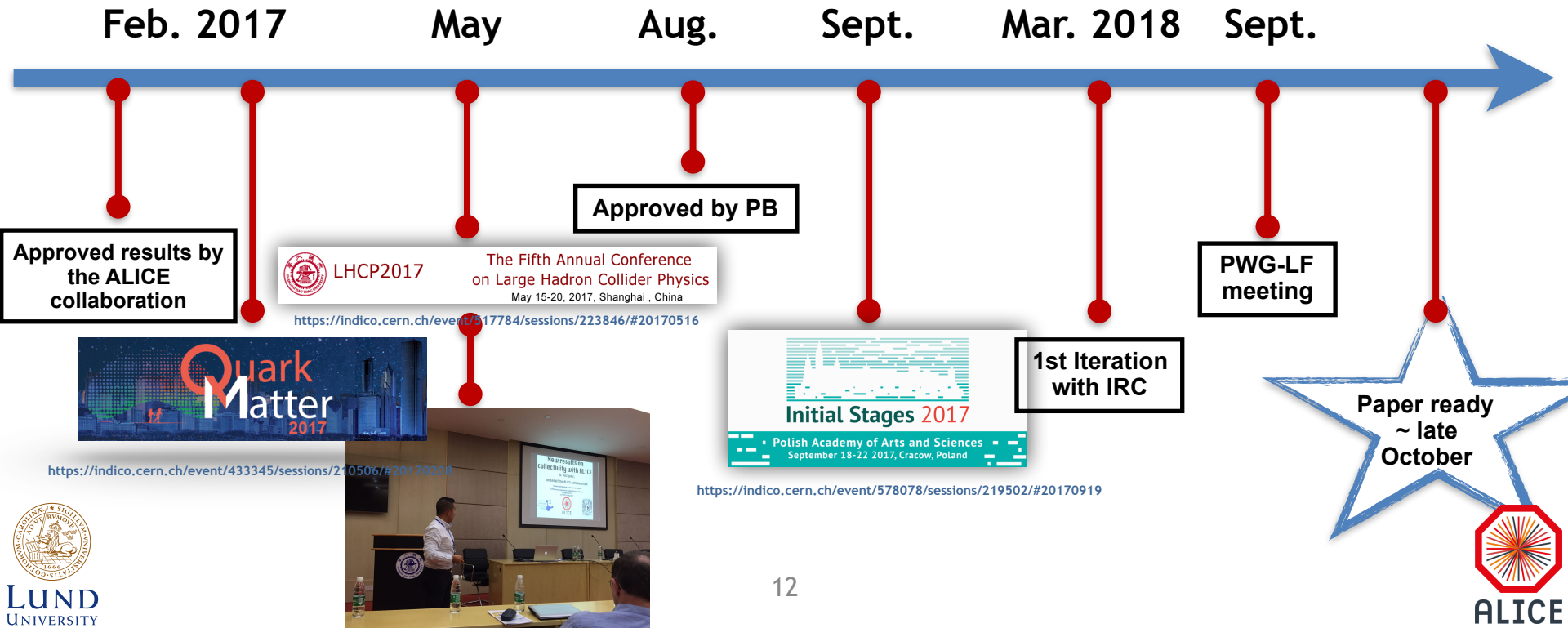


$$\left(\frac{K^+ + K^-}{2} \right) / K_S^0$$

Combined



Production of charged pions, kaons (anti)protons in Pb—Pb and minimum bias pp collisions at 5.02 TeV



Production of charged pions, kaons (anti)protons in Pb—Pb and minimum bias pp at collisions at 5.02 TeV

ID number: 3828

e-group: [alice-paperdraft-id3828](#)

PWG: PWG-LF (Light Flavour Spectra)

Format: Regular Paper

Approved by PB: 30 August, 2017

Paper Committee members: Giacomo Volpe

Yasser Corrales Morales

Nur Hussain

Nicolo Jacazio

Antonio Ortiz Velasquez

Ivan Ravasenga

Omar Vazquez Rueda

Paper Committee members's email: Giacomo.Volpe@cern.ch

yasser.corrales.morales@cern.ch

nur.hussain@cern.ch

nicolo.jacazio@cern.ch

Antonio.Ortiz.Velasquez@cern.ch

ivan.ravasenga@cern.ch

omar.vazquez.rueda@cern.ch

IRC Members: Peter Christiansen

Christina Markert

Jacek Tomasz Otwinowski

EUROPEAN ORGANIZATION FOR NUCLEAR RESEARCH



CERN-EP-2018-XXX
25 May 2018

Production of charged pions, kaons and (anti)protons in Pb—Pb and minimum bias pp collisions at $\sqrt{s_{NN}} = 5.02$ TeV

ALICE Collaboration^a

Abstract

In this paper, the mid-rapidity ($|y| < 0.5$) production of π^{\pm} , K^{\pm} and $p(\bar{p})$ in Pb—Pb and minimum bias pp collisions at $\sqrt{s_{NN}} = 5.02$ TeV is presented. The invariant yields are measured over a wide transverse momentum (p_T) range from hundreds of MeV/c up to 20 GeV/c. The results in Pb—Pb collisions are presented as a function of the collision centrality. The comparison of the p_T -integrated particle ratios, i.e. proton-to-pion and kaon-to-pion ratios, with analogous measurements in Pb—Pb collisions at $\sqrt{s_{NN}} = 2.76$ TeV show no significant energy dependence. However, particle ratios as a function of p_T show distinctive maxima at $p_T \approx 3$ GeV/c in central Pb—Pb collisions. Their positions slightly depend on energy. In particular for the proton-to-pion ratio. The blast-wave analysis of the p_T spectra gives an average transverse expansion velocity of $\langle \beta_T \rangle \approx 0.663 \pm 0.004$, indicating that radial flow is slightly higher than that measured at $\sqrt{s_{NN}} = 2.76$ TeV ($\langle \beta_T \rangle \approx 0.651$). Using the pp reference spectra measured at the same collision energy of 5.02 TeV, the nuclear modification factors for the different particle species are derived. Within uncertainties, the nuclear modification factor is particle species independent for $p_T > 10$ GeV/c and compatible with measurements at $\sqrt{s_{NN}} = 2.76$ TeV. The results are compared with theoretical predictions.

© 2018 CERN for the benefit of the ALICE Collaboration.

Reproduction of this article or parts of it is allowed as specified in the [CC-BY-4.0 license](#).

^aSee Appendix B for the list of collaboration members

$\pi/K/p$ production in Pb–Pb and MB pp collisions at $\sqrt{s_{NN}} = 5.02$ TeV ALICE Collaboration

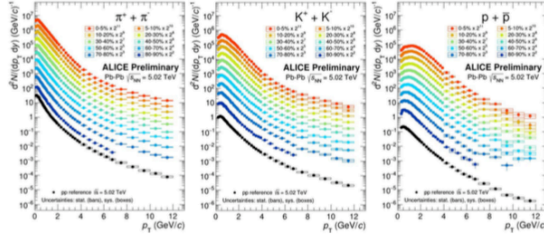


Fig. 3: Transverse momentum spectra of pions (left), kaons (middle) and protons (right) measured in Pb–Pb collisions at $\sqrt{s_{NN}} = 5.02$ TeV for different centrality classes. Scale factors are applied for better visibility. The results are compared with the spectra measured in minimum-bias pp collisions at $\sqrt{s} = 5.02$ TeV. Statistical and systematic uncertainties are displayed as error bars and boxes around the data points, respectively.

3.1 Particle production at low transverse momentum

In order to quantify the centrality dependent change of the spectral shapes at low p_T (< 2 – 3 GeV/c) the Boltzmann-Gibbs blast-wave function [66], reported in Eq. 1, has been simultaneously fitted to the charged pion, kaon and (anti)proton spectra.

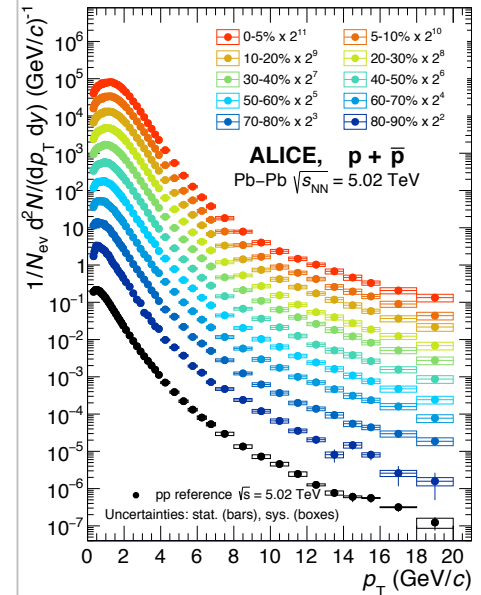
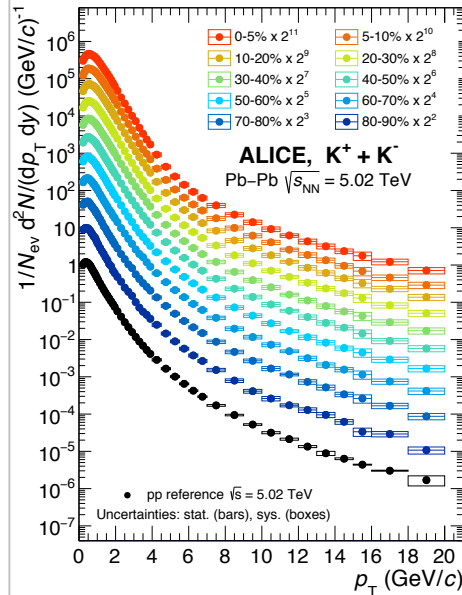
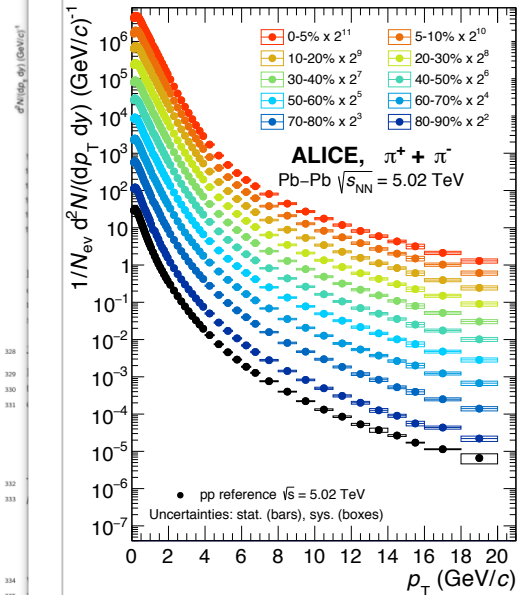
$$E \frac{d^3N}{d^3p^2} \propto \int_0^R m_T l_0 \left(\frac{p_T \sinh(\rho)}{T_{kin}} \right) K_1 \left(\frac{m_T \cosh(\rho)}{T_{kin}} \right) r dr \quad (3)$$

The blast-wave function is a three parameters simplified hydrodynamic model where the velocity profile ρ is given by:

$$\rho = \tanh^{-1} \beta_T = \tanh^{-1} \left(\left(\frac{r}{R} \right)^\alpha \beta_s \right) \quad (4)$$

where β_T is the radial expansion velocity, m_T the transverse mass ($m_T = \sqrt{m^2 + p_T^2}$) and T_{kin} the temperature at the kinetic freeze-out. Although the absolute values of the parameters have a strong dependence on the fitting range used in the analysis, it still makes sense to compare the evolution of the parameters with $\sqrt{s_{NN}}$ when the fits are done within the same p_T intervals. In the present analysis we used the same p_T intervals employed in a previous publication [15], namely, 0.5–1 GeV/c, 0.2–1.5 GeV/c and 0.3–3 GeV/c for charged pions, kaons and (anti)protons, respectively. Figure 4 shows the ratios of the spectra to the combined fits for all the centrality classes and particle species. If the behavior of the spectra over the full p_T range would be purely hydrodynamic, then the fitted functions determined within a limited p_T range would be expected to describe the spectral shape in the full p_T range. This is only observed for the proton and kaon p_T spectra in 0–20% Pb–Pb collisions. A different situation is observed for pions where, due to their smaller masses and feed down from resonance decays, the agreement with the model is worse than that observed for kaons and (anti-)protons. The p_T threshold at which the function deviates from the data increases with increasing the impact parameter, indicating the need for more sophisticated hydrodynamic implementations.

Particle production at low p_T



the same p_T intervals employed in a previous publication [15], namely, 0.5 – 1 GeV/c, 0.2 – 1.5 GeV/c and 0.3 – 3 GeV/c for charged pions, kaons and (anti)protons, respectively. Figure 4 shows the ratios of the spectra to the combined fits for all the centrality classes and particle species. If the behavior of the spectra over the full p_T range would be purely hydrodynamic, then the fitted functions determined within a limited p_T range would be expected to describe the spectral shape in the full p_T range. This is only observed for the proton and kaon p_T spectra in 0-20% Pb–Pb collisions. A different situation is observed for pions where, due to their smaller masses and feed down from resonance decays, the agreement with the model is worse than that observed for kaons and (anti-)protons. The p_T threshold at which the function deviates from the data increases with increasing the impact parameter, indicating the need for more sophisticated hydrodynamic implementations.

- The full p_T spectra is a combined result of independent PID techniques: ITS, TPC, TOF, HMPID and kaons identification from kinks.
- Going from peripheral to central Pb-Pb collisions the spectra exhibit a flattening at low p_T (~ 1 GeV/c), the effect is more pronounced for heavier particles. This behavior is consistent with the presence of radial flow.

Intermediate p_T

$\pi/K/p$ production in Pb–Pb and MB pp collisions at $\sqrt{s_{NN}} = 5.02$ TeV ALICE Collaboration

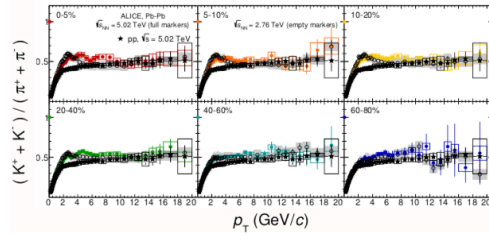


Fig. 8: Centrality dependence of the K/π ratio as a function of transverse momentum, measured in Pb–Pb collisions at $\sqrt{s_{NN}} = 5.02$ and 2.76 TeV. The ratio in pp collisions at $\sqrt{s} = 5.02$ TeV is also shown. The statistical and systematic uncertainties are shown as error bars and boxes around the data points, respectively.

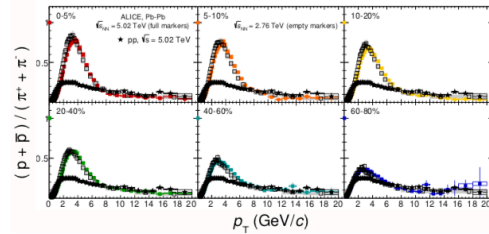
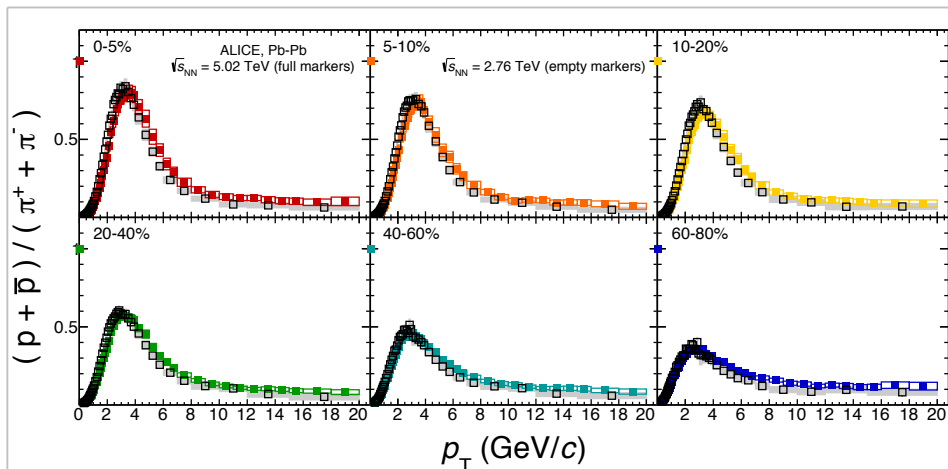
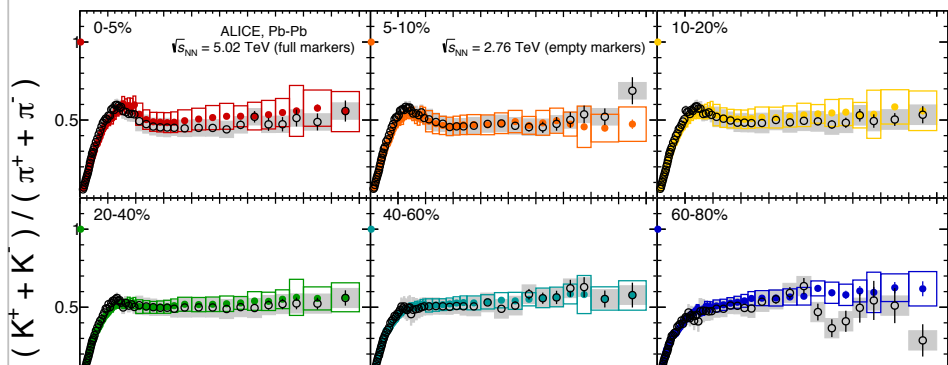


Fig. 9: Centrality dependence of the p/π ratio as a function of transverse momentum, measured in Pb–Pb collisions at $\sqrt{s_{NN}} = 5.02$ and 2.76 TeV. The ratio in pp collisions at $\sqrt{s} = 5.02$ TeV is also shown. The statistical and systematic uncertainties are shown as error bars and boxes around the data points, respectively.

396 Figure 9 shows the proton-to-pion (p/π) ratio as a function of p_T . The ratios measured in heavy-ion
 397 collisions exhibit a pronounced enhancement with respect to minimum-bias pp collisions, reaching a
 398 value of about 0.9 at $p_T = 3$ GeV/c. This is reminiscent of the increase in the baryon-to-meson ratio
 399 observed at RHIC in the intermediate p_T region [74]. Such an increase with p_T is an intrinsic feature of
 400 hydrodynamic models, where it is due to the mass ordering induced by radial flow (heavier particles are
 401 boosted to higher p_T by the collective motion). It should be noted, however, that this is also suggestive
 402 of the recombination picture as discussed in the introduction. However, since recombination is a baryon
 403 effect, it would not explain the bump which is also observed in the kaon-to-pion ratio. Because in Pb–Pb
 404 collisions at $\sqrt{s_{NN}} = 5.02$ TeV the radial flow was found to be higher than at $\sqrt{s_{NN}} = 2.76$ TeV, we can

Intermediate p_T



□ In the proton-to-pion ratio, the shift of the peak toward higher values of p_T indicates a signature of stronger radial flow compared to Pb—Pb collisions at $\sqrt{s_{NN}} = 2.76$ TeV.

Particle production at high p_T

$\pi/K/p$ production in Pb–Pb and MB pp collisions at $\sqrt{s_{NN}} = 5.02$ TeV ALICE Collaboration

understand that the p/π bump is located at higher p_T in 5.02 TeV data. Finally, both particle ratios
for $p_T > 10$ GeV/c become similar to 2.76 TeV and behave like those in pp collisions, suggesting that
vacuum-like fragmentation processes dominated there [27].

3.3 Particle production at high transverse momentum

Figure 10 shows the centrality dependence of R_{AA} as a function of p_T for charged pions, kaons and
(anti)protons. For $p_T < 10$ GeV/c protons appear to be less suppressed than kaons and pions, consistent
with the particle ratios shown in Fig. 9. At larger p_T (> 10 GeV/c) all particle species are equally
suppressed; so despite the strong energy loss observed in the most central heavy-ion collisions, the
particle composition and ratios at high p_T are similar to those in vacuum. This suggests that jet quenching
does not produce signatures that affect the particle species composition for the leading particles. It is
worth mentioning two interesting features of the unidentified-charged particle production [75] which has
been measured up to 300 GeV/c [37]. Firstly, as seen in the identified particle results a gradual approach
of R_{AA} to unity is observed going from central to 60–80% Pb–Pb collisions. Secondly, for central Pb–Pb
collisions the results for unidentified charged particles gives an R_{AA} which reaches unity for p_T higher
than 100 GeV/c. The second effect can not be seen in the pion, kaon and (anti-)proton analysis due
to limited p_T reach. However, based on inclusive charged particle R_{AA} results, the R_{AA} of identified

particles is also expected to increase up unity for very high p_T .

Concerning the behavior of the identified-particle R_{AA} for peripheral Pb–Pb collisions, namely, the
apparent presence of jet quenching ($R_{AA} < 1$) though for similar particle densities in smaller systems (like
p-Pb collisions) no jet quenching signatures have been reported [76]. It has been argued that peripheral
A-A collisions can be significantly affected by event selection and geometry biases [77] leading to an
apparent suppression for R_{AA} even if jet quenching and shadowing are absent. The presence of the biases
in heavy-ion data has been confirmed by means of the measurement of R_{AA} for very peripheral Pb–Pb
collisions [78]. All hard probes should be similarly affected [77], in particular the leading pions, kaons
and protons reported in the present paper.

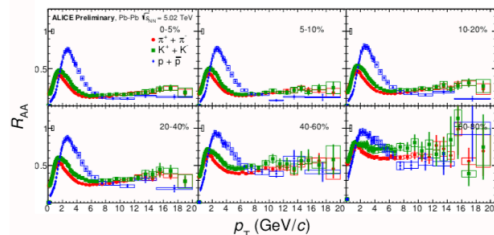
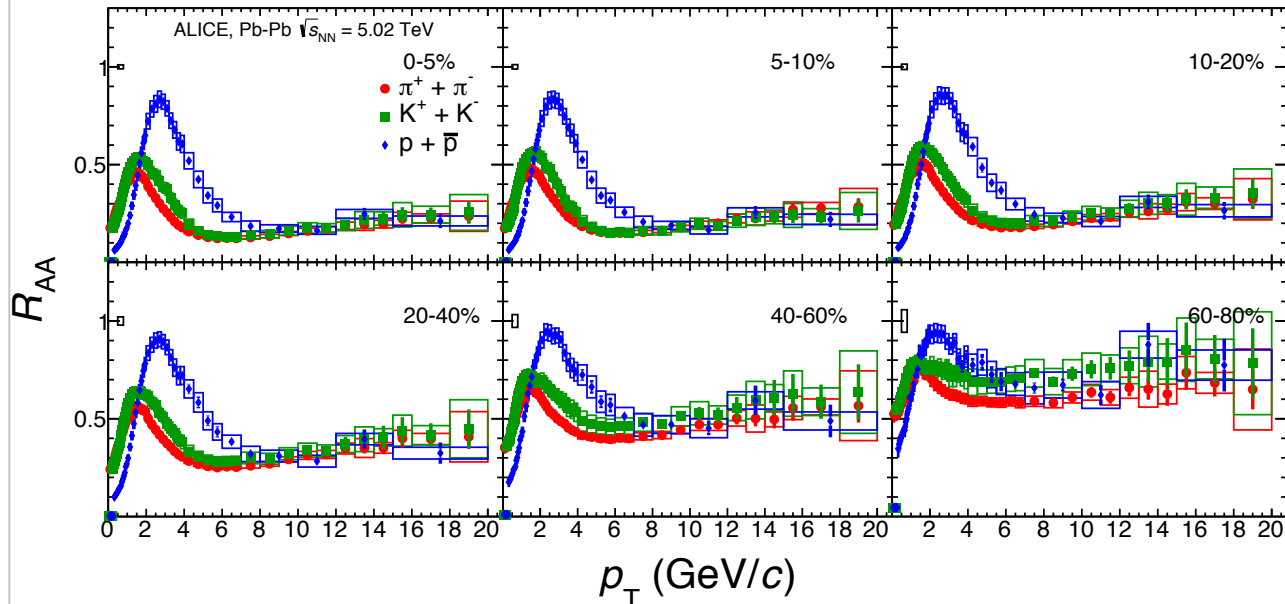


Fig. 10: Centrality dependence of the nuclear modification factor of charged π^+ , K^+ and p (p) as a function of transverse momentum, measured in Pb–Pb collisions at $\sqrt{s_{NN}} = 5.02$ TeV. The statistical and systematic uncertainties are shown as error bars and boxes around the data points.

Figure 11 shows the R_{AA} for charged pions, kaons and (anti)protons for central (0–5%) and peripheral
(60–80%) Pb–Pb collisions at $\sqrt{s_{NN}} = 2.76$ TeV and $\sqrt{s_{NN}} = 5.02$ TeV. No significant dependence

Particle production at high p_T



$\pi/K/p$ production in Pb–Pb and MB

understand that the p/π bump is local
for $p_T > 10$ GeV/c become similar to
vacuum-like fragmentation processes

3.3 Particle production at high p_T

Figure 10 shows the centrality dependence of R_{AA} for π^\pm and p/\bar{p} . For $p_T < 10$ GeV/c R_{AA} is suppressed, so despite the strong centrality dependence of the particle ratios at high p_T does not produce signatures that are worth mentioning two interesting features have been measured up to 300 GeV/c [37].

of R_{AA} to unity is observed going from peripheral collisions the results for unidentified particles are shown in Figure 11.

Concerning the behavior of the identified particles in heavy-ion collisions the apparent presence of jet quenching ($R_{AA} < 1$) in p-Pb collisions no jet quenching signature is observed. A-A collisions can be significantly different from p-Pb collisions even if the apparent suppression for R_{AA} even if it is in heavy-ion data has been confirmed in collisions [78]. All hard probes should be compared to the results for pions and protons reported in the present paper.

ALICE Preliminary, Pb–Pb $\sqrt{s_{NN}} = 5.02$ TeV

0–5%
 $\pi^+ + \pi^-$
 $K^+ + K^-$
 $p + \bar{p}$

20–40%

60–80%

0–5%
 $\pi^+ + \pi^-$
 $K^+ + K^-$
 $p + \bar{p}$

20–40%

60–80%

0–5%
 $\pi^+ + \pi^-$
 $K^+ + K^-$
 $p + \bar{p}$

20–40%

60–80%

0–5%
 $\pi^+ + \pi^-$
 $K^+ + K^-$
 $p + \bar{p}$

20–40%

60–80%

0–5%
 $\pi^+ + \pi^-$
 $K^+ + K^-$
 $p + \bar{p}$

20–40%

60–80%

0–5%
 $\pi^+ + \pi^-$
 $K^+ + K^-$
 $p + \bar{p}$

20–40%

60–80%

0–5%
 $\pi^+ + \pi^-$
 $K^+ + K^-$
 $p + \bar{p}$

20–40%

60–80%

0–5%
 $\pi^+ + \pi^-$
 $K^+ + K^-$
 $p + \bar{p}$

20–40%

60–80%

0–5%
 $\pi^+ + \pi^-$
 $K^+ + K^-$
 $p + \bar{p}$

20–40%

60–80%

0–5%
 $\pi^+ + \pi^-$
 $K^+ + K^-$
 $p + \bar{p}$

20–40%

60–80%

0–5%
 $\pi^+ + \pi^-$
 $K^+ + K^-$
 $p + \bar{p}$

20–40%

60–80%

0–5%
 $\pi^+ + \pi^-$
 $K^+ + K^-$
 $p + \bar{p}$

20–40%

60–80%

0–5%
 $\pi^+ + \pi^-$
 $K^+ + K^-$
 $p + \bar{p}$

20–40%

60–80%

0–5%
 $\pi^+ + \pi^-$
 $K^+ + K^-$
 $p + \bar{p}$

20–40%

60–80%

0–5%
 $\pi^+ + \pi^-$
 $K^+ + K^-$
 $p + \bar{p}$

20–40%

60–80%

0–5%
 $\pi^+ + \pi^-$
 $K^+ + K^-$
 $p + \bar{p}$

20–40%

60–80%

0–5%
 $\pi^+ + \pi^-$
 $K^+ + K^-$
 $p + \bar{p}$

20–40%

60–80%

0–5%
 $\pi^+ + \pi^-$
 $K^+ + K^-$
 $p + \bar{p}$

20–40%

60–80%

0–5%
 $\pi^+ + \pi^-$
 $K^+ + K^-$
 $p + \bar{p}$

20–40%

60–80%

0–5%
 $\pi^+ + \pi^-$
 $K^+ + K^-$
 $p + \bar{p}$

20–40%

60–80%

0–5%
 $\pi^+ + \pi^-$
 $K^+ + K^-$
 $p + \bar{p}$

20–40%

60–80%

0–5%
 $\pi^+ + \pi^-$
 $K^+ + K^-$
 $p + \bar{p}$

20–40%

60–80%

0–5%
 $\pi^+ + \pi^-$
 $K^+ + K^-$
 $p + \bar{p}$

20–40%

60–80%

0–5%
 $\pi^+ + \pi^-$
 $K^+ + K^-$
 $p + \bar{p}$

20–40%

60–80%

0–5%
 $\pi^+ + \pi^-$
 $K^+ + K^-$
 $p + \bar{p}$

20–40%

60–80%

0–5%
 $\pi^+ + \pi^-$
 $K^+ + K^-$
 $p + \bar{p}$

20–40%

60–80%

0–5%
 $\pi^+ + \pi^-$
 $K^+ + K^-$
 $p + \bar{p}$

20–40%

60–80%

0–5%
 $\pi^+ + \pi^-$
 $K^+ + K^-$
 $p + \bar{p}$

20–40%

60–80%

0–5%
 $\pi^+ + \pi^-$
 $K^+ + K^-$
 $p + \bar{p}$

20–40%

60–80%

0–5%
 $\pi^+ + \pi^-$
 $K^+ + K^-$
 $p + \bar{p}$

20–40%

60–80%

0–5%
 $\pi^+ + \pi^-$
 $K^+ + K^-$
 $p + \bar{p}$

20–40%

60–80%

0–5%
 $\pi^+ + \pi^-$
 $K^+ + K^-$
 $p + \bar{p}$

20–40%

60–80%

0–5%
 $\pi^+ + \pi^-$
 $K^+ + K^-$
 $p + \bar{p}$

20–40%

60–80%

0–5%
 $\pi^+ + \pi^-$
 $K^+ + K^-$
 $p + \bar{p}$

20–40%

60–80%

0–5%
 $\pi^+ + \pi^-$
 $K^+ + K^-$
 $p + \bar{p}$

20–40%

60–80%

0–5%
 $\pi^+ + \pi^-$
 $K^+ + K^-$
 $p + \bar{p}$

20–40%

60–80%

0–5%
 $\pi^+ + \pi^-$
 $K^+ + K^-$
 $p + \bar{p}$

20–40%

60–80%

0–5%
 $\pi^+ + \pi^-$
 $K^+ + K^-$
 $p + \bar{p}$

20–40%

60–80%

0–5%
 $\pi^+ + \pi^-$
 $K^+ + K^-$
 $p + \bar{p}$

20–40%

60–80%

0–5%
 $\pi^+ + \pi^-$
 $K^+ + K^-$
 $p + \bar{p}$

20–40%

60–80%

0–5%
 $\pi^+ + \pi^-$
 $K^+ + K^-$
 $p + \bar{p}$

20–40%

60–80%

0–5%
 $\pi^+ + \pi^-$
 $K^+ + K^-$
 $p + \bar{p}$

20–40%

60–80%

0–5%
 $\pi^+ + \pi^-$
 $K^+ + K^-$
 $p + \bar{p}$

20–40%

60–80%

0–5%
 $\pi^+ + \pi^-$
 $K^+ + K^-$
 $p + \bar{p}$

20–40%

60–80%

0–5%
 $\pi^+ + \pi^-$
 $K^+ + K^-$
 $p + \bar{p}$

20–40%

60–80%

0–5%
 $\pi^+ + \pi^-$
 $K^+ + K^-$
 $p + \bar{p}$

20–40%

60–80%

0–5%
 $\pi^+ + \pi^-$
 $K^+ + K^-$
 $p + \bar{p}$

20–40%

60–80%

0–5%
 $\pi^+ + \pi^-$
 $K^+ + K^-$
 $p + \bar{p}$

20–40%

60–80%

0–5%
 $\pi^+ + \pi^-$
 $K^+ + K^-$
 $p + \bar{p}$

20–40%

60–80%

0–5%
 $\pi^+ + \pi^-$
 $K^+ + K^-$
 $p + \bar{p}$

20–40%

60–80%

0–5%
 $\pi^+ + \pi^-$
 $K^+ + K^-$
 $p + \bar{p}$

20–40%

60–80%

0–5%
 $\pi^+ + \pi^-$
 $K^+ + K^-$
 $p + \bar{p}$

20–40%

60–80%

0–5%
 $\pi^+ + \pi^-$
 $K^+ + K^-$
 $p + \bar{p}$

20–40%

60–80%

0–5%
 $\pi^+ + \pi^-$
 $K^+ + K^-$
 $p + \bar{p}$

20–40%

60–80%

0–5%
 $\pi^+ + \pi^-$
 $K^+ + K^-$
 $p + \bar{p}$

20–40%

60–80%

0–5%
 $\pi^+ + \pi^-$
 $K^+ + K^-$
 $p + \bar{p}$

20–40%

60–80%

0–5%
 $\pi^+ + \pi^-$
 $K^+ + K^-$
 $p + \bar{p}$

20–40%

60–80%

0–5%
 $\pi^+ + \pi^-$
 $K^+ + K^-$
 $p + \bar{p}$

20–40%

60–80%

0–5%
 $\pi^+ + \pi^-$
 $K^+ + K^-$
 $p + \bar{p}$

20–40%

60–80%

0–5%
 $\pi^+ + \pi^-$
 $K^+ + K^-$
 $p + \bar{p}$

20–40%

60–80%

0–5%
 $\pi^+ + \pi^-$
 $K^+ + K^-$
 $p + \bar{p}$

20–40%

60–80%

0–5%
 $\pi^+ + \pi^-$
 $K^+ + K^-$
 $p + \bar{p}$

20–40%

60–80%

0–5%
 $\pi^+ + \pi^-$
 $K^+ + K^-$
 $p + \bar{p}$

20–40%

60–80%

0–5%
 $\pi^+ + \pi^-$
 $K^+ + K^-$
 $p + \bar{p}$

20–40%

60–80%

0–5%
 $\pi^+ + \pi^-$
 $K^+ + K^-$
 $p + \bar{p}$

20–40%

60–80%

0–5%
 $\pi^+ + \pi^-$
 $K^+ + K^-$
 $p + \bar{p}$

20–40%

60–80%

0–5%
 $\pi^+ + \pi^-$
 $K^+ + K^-$
 $p + \bar{p}$

20–40%

60–80%

0–5%
 $\pi^+ + \pi^-$
 $K^+ + K^-$
 $p + \bar{p}$

20–40%

60–80%

0–5%
 $\pi^+ + \pi^-$
 $K^+ + K^-$
 $p + \bar{p}$

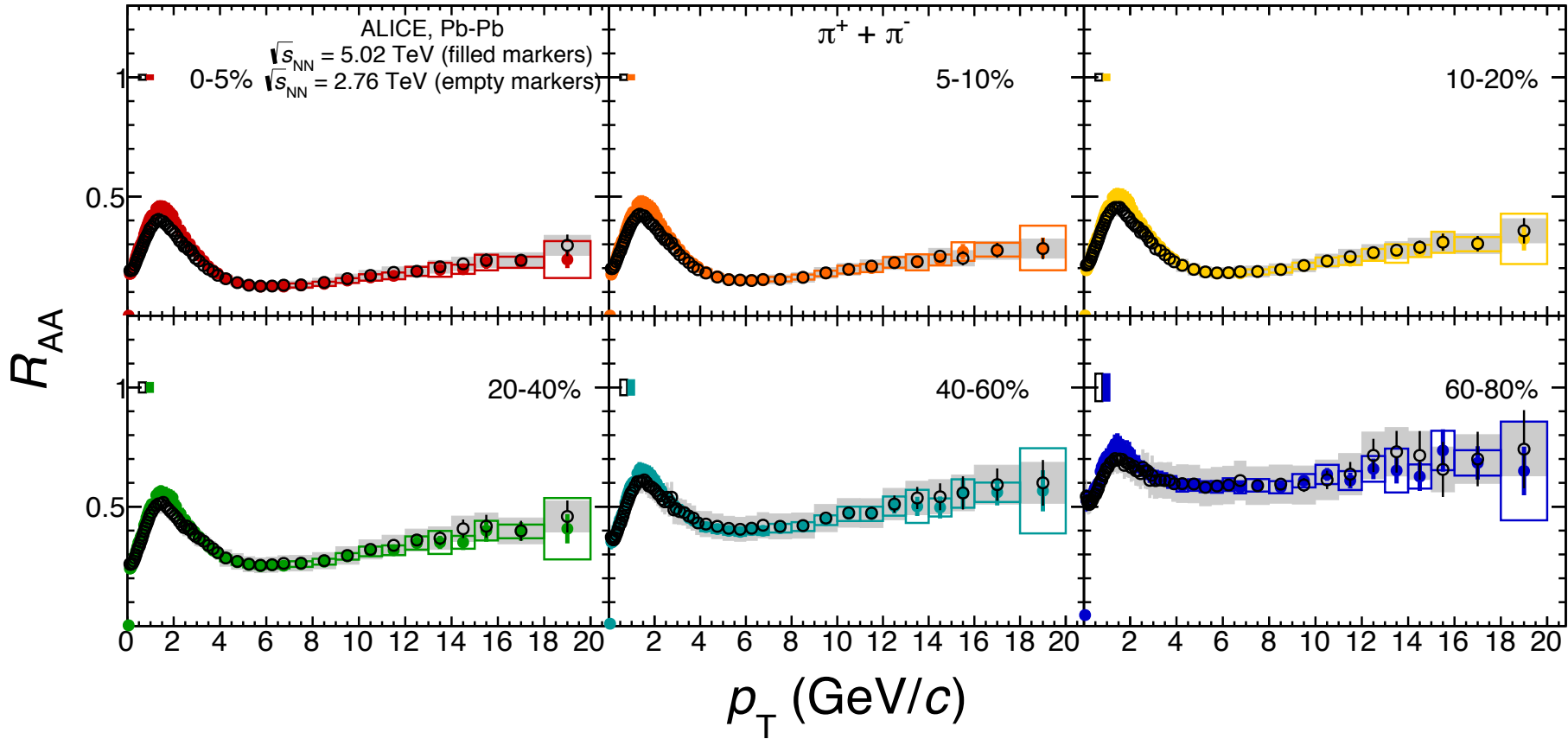
20–40%

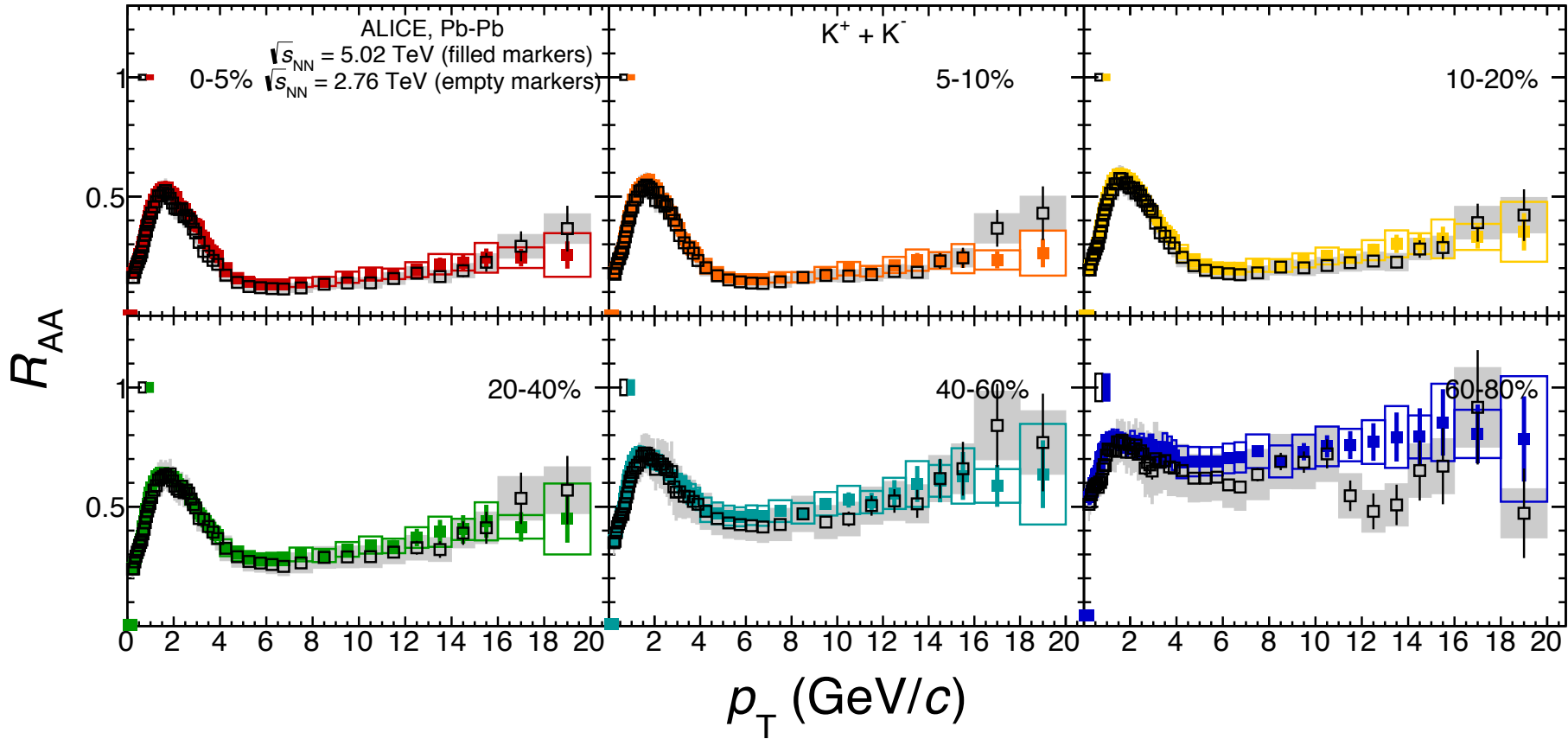
60–80%

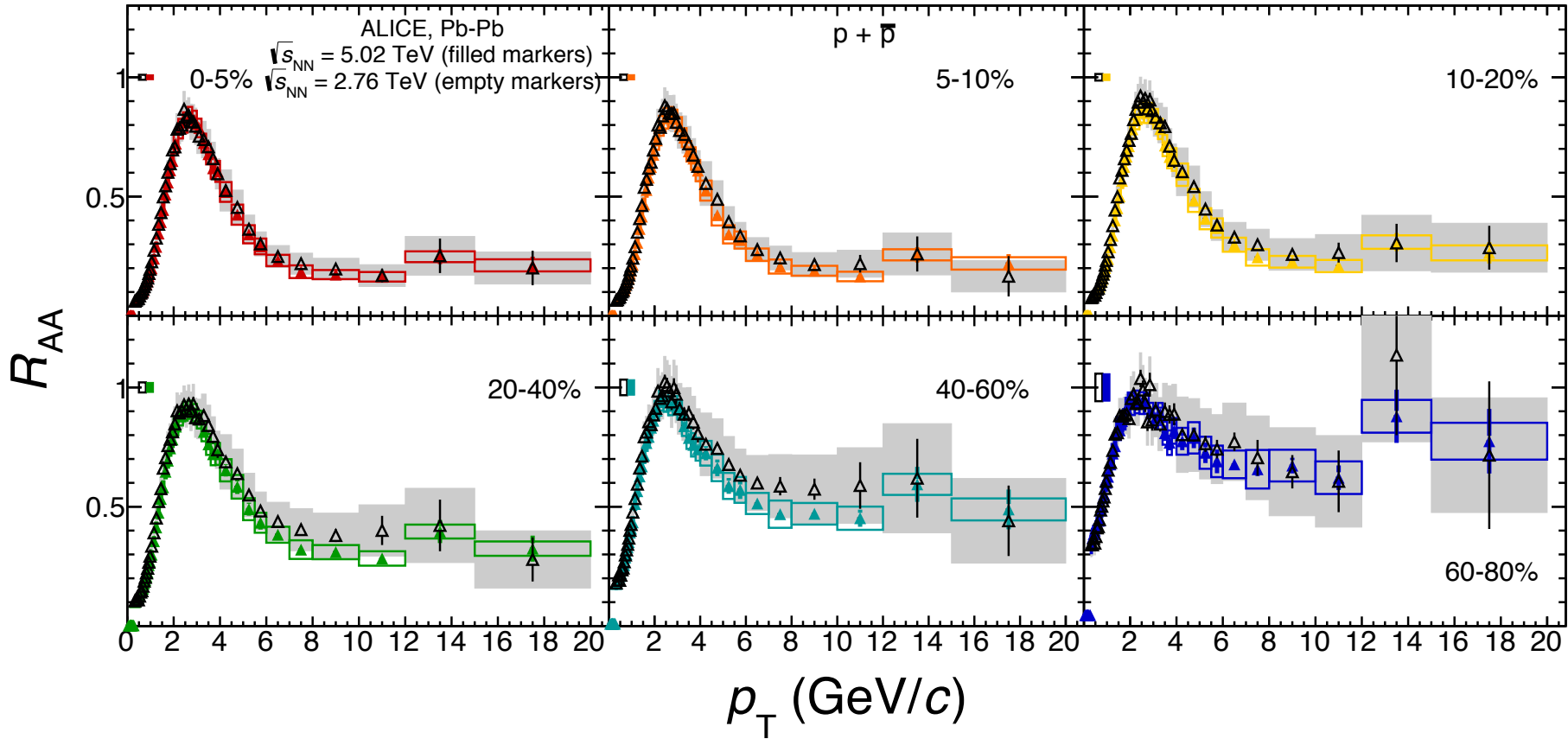
Conclusions

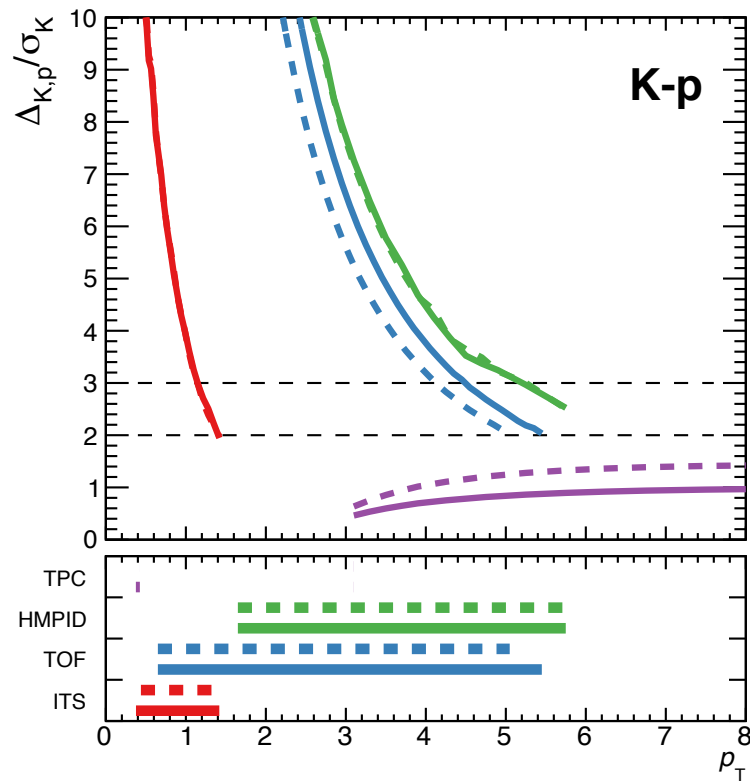
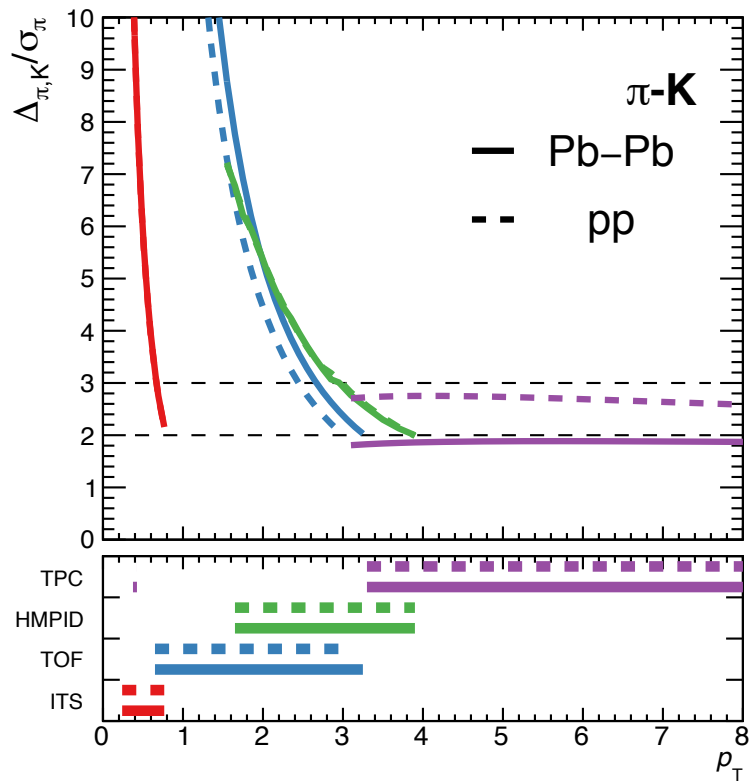
- We have observed an increase of radial flow compared to Pb—Pb collisions at 2.76 TeV.
- No significant evolution of nuclear modification at high- p_T with the center of mass energy is observed.
- The publication of the “Production of charged pions, kaons, (anti)protons in Pb—Pb and minimum bias pp collisions at 5.02 TeV” paper is approaching fast !!

Backup









❖ Separation power of hadron identification.

Power law exponent

